

# Comparison of the MRI and Integrated PET/CT Findings in the Preoperative Detection of Peritoneal Carcinomatosis Arising from Primary Ovarian Cancer<sup>1</sup>

Chan Kyo Kim, M.D., Byung Kwan Park, M.D., Joon Young Choi, M.D.<sup>2</sup>, Ji Hye Kim, M.D.

**Purpose:** To compare the diagnostic performance of MRI and integrated PET/CT for the preoperative detection of peritoneal carcinomatosis arising from primary ovarian cancer.

**Materials and Methods:** Twenty-three patients with suspected ovarian tumors underwent a contrast-enhanced 1.5 Tesla MRI and a 18F-fluorodeoxyglucose (FDG) PET/CT prior to surgery. The peritoneal cavity was subdivided into six specific sites for a lesion-based analysis. The imaging findings were compared statistically with the histopathological findings using McNemar's test with Bonferroni's adjustment and generalized estimation equations.

**Results:** The histopathological results of all 23 patients were confirmed for primary malignant epithelial ovarian cancer. Of the 23 patients, 19 had a total of 83 sites with peritoneal seedings throughout the abdomen and pelvis. The comparison of the patient-based sensitivity, specificity and accuracy of the use of MRI versus PET/CT for the detection of peritoneal carcinomatosis were 95% versus 84% ( $p > 0.05$ ; N.S.), 50% versus 50% ( $p > 0.05$ ; N.S.), and 87% versus 78% ( $p > 0.05$ ; N.S.), respectively. Moreover, the comparison of the lesion-based sensitivity, specificity and accuracy of MRI versus integrated PET/CT were 86% and 75% ( $p = 0.004$ ), 76% and 84% ( $p > 0.05$ ; N.S.), and 82% and 78% ( $p > 0.05$ ; N.S.), respectively.

**Conclusion:** We found that MRI was more sensitive than integrated PET/CT for the detection of preoperative peritoneal carcinomatosis arising from primary ovarian cancer.

**Index words :** Ovary, neoplasm  
Magnetic resonance (MR)  
Positron emission tomography  
Peritoneum, neoplasm  
Ovarian cancer, staging

<sup>1</sup>Department of Radiology and Center for Imaging Science, Samsung Medical Center, Sungkyunkwan University School of Medicine

<sup>2</sup>Department of Nuclear Medicine, Samsung Medical Center, Sungkyunkwan University, School of Medicine

Received May 25, 2008 ; Accepted September 19, 2008

Address reprint requests to : Chan Kyo Kim, M.D., Department of Radiology, Samsung Medical Center, 50 Irwon-dong, Kangnam-gu, Seoul 135-710, Korea  
Tel. 82-2-3410-0516 Fax. 82-2-3410-2559 E-mail: chankyokim@skku.edu

Epithelial ovarian cancer is the most common gynecological malignancy and the ninth most frequent cause of cancer-related death in women. In South Korea, an estimated 1,334 new cases of ovarian cancer per year were diagnosed from 1999 to 2002, along with an estimated 717 deaths in 2006 (1, 2). For ovarian cancer, 75% of patients present with advanced disease (stage III or IV) and in 60% of patients, the cancer spread exceeds the pelvis (3). In addition to the infiltration of the neighboring organs and invasion of the lymph and blood vessels, secondary dissemination of tumor cells following the path of peritoneal fluid, is also characteristic of advanced ovarian carcinoma (4, 5).

The presence of a peritoneal tumor alters tumor staging and has implications for primary treatment and patient outcome. Peritoneal seeding is one of the most important prognostic indicators in ovarian cancer (6). In patients with advanced ovarian cancer, CT or magnetic resonance imaging (MRI) may be used to detect peritoneal implants greater than 1–2 cm at critical unresectable sites and can thus predict suboptimal cytoreduction (7). The results of the detection for peritoneal seeding using CT or MRI have been reported to have accuracies ranging from 82–95% (8–18). Some studies have shown that MRI is more sensitive than CT to predict peritoneal seeding due to the high spatial resolution between the enhancing peritoneum and adjacent structures (10, 11, 17).

The role of the use of PET in ovarian cancer has not yet been defined. Some investigations have shown that the use of PET does not improve the diagnostic accuracy, while others have shown that PET can supplement the information obtained by CT and MRI (19–23). Some recent studies have demonstrated that for peritoneal carcinomatosis, the use of combined PET and CT may play an important role in the clinical management of patients (24, 25). However, to the best of our knowledge, there are few reports that have examined a comparison of the use of MRI and integrated PET/CT to predict the presence of peritoneal carcinomatosis resulting from primary ovarian cancer (26).

The purpose of this study was to compare the use of MRI versus the integrated PET/CT for the preoperative prediction of peritoneal carcinomatosis arising from ovarian cancer.

## Materials and Methods

### Study Population

Between March 2003 and January 2006, a total of 253 patients underwent a staging laparotomy with tumor debulking. Of these patients, 198 underwent a preoperative MRI examination alone, whereas 32 underwent a preoperative PET/CT examination alone. A total of 23 patients (mean age,  $60 \pm 1.8$  years; age range, 34–79 years) underwent both fluorodeoxyglucose (FDG) PET/CT and MRI, and were enrolled in this study. The interval between the two studies was less than four weeks. For all patients the presence or absence of peritoneal carcinomatosis was established with the use of a staging laparotomy in accordance with the International Federation of Obstetrics and Gynecology surgical staging system for ovarian cancer. Staging laparotomies in all 23 patients were performed by two gynecologic surgeons. The interval between the staging laparotomy and MRI examination ranged from 5 to 30 days (mean: 22 days). Moreover, the interval between the staging laparotomy and PET/CT examination ranged from 10 to 27 days (mean: 18 days). Of the 23 patients with malignant ovarian cancer, 17 had stage III (stage IIIB,  $n = 6$ ; stage IIIC,  $n = 11$ ) and two had stage IV with peritoneal carcinomatosis. The remaining four patients did not have peritoneal carcinomatosis (stage IIA,  $n = 2$ ; stage IIB,  $n = 2$ ).

All cases of peritoneal spread were confirmed by surgical findings and a histological view of the omentectomy, as well as debulking. A final histopathological analysis of the ovarian cancer identified 20 serous adenocarcinomas, two endometrioid adenocarcinomas, and one mixed epithelial tumor. Our institutional review board approved this study and waived the patient informed consent, as the study was a retrospective analysis.

### MR Imaging Protocol

MRI was performed on all 23 patients using a 1.5-Tesla MR system (Signa; GE Medical Systems, Milwaukee, WI U.S.A.) with a phased array or body coil. The phased array was used for pelvic imaging and the body coil was used for abdominal imaging. However, the body coil alone was used for imaging the pelvis and abdomen in the presence of a mass larger than 15 cm in diameter or for a patient with severe obesity or ascites. All of the patients were requested to fast for at least six hours before MR imaging and were ad-

ministered 20 mg of butyl scopolamine (Buscopan, Boehringer Ingelheim, Ingelheim am Rhein, Germany) intramuscularly before the MR imaging (unless the use of the drug was contraindicated). No bowel preparation or oral contrast material was administered.

The pelvis was imaged with an axial fast spin-echo T2-weighted sequence (5,000–6,000/102–126 repetition time msec/echo time msec) with an echo train length of 16, a 5–7 mm section thickness and a 0–2.5 mm inter-section gap. The matrix was  $512 \times 256$  with the two signals acquired. This sequence was repeated in the coronal and sagittal planes. Next, an axial T1-weighted spin-echo sequence (600–800/11–20) with a spatial resolution similar to that of the T2-weighted sequence was performed. The T1-weighted sequence was repeated with and without fat suppression after the administration of a bolus injection of gadopentetate dimeglumine (Magnevist, Schering, Berlin, Germany) at a rate of 2 mL/s and a dose level of 0.1 mmol/kg body weight using a power injector.

The remainder of the abdomen and pelvis was imaged with a delayed post-contrast axial T2-weighted fast spin-echo sequence and an axial T1-weighted spin-echo sequence, with and without fat-suppression. The T2-weighted sequence (4,000/102–126) had an echo train length of 16, an 8–10 mm section thickness, and a 1.0–2.5 mm gap. The matrix measured  $256 \times 192$  with two to four signals acquired. This sequence was repeated in the coronal and sagittal planes. The T1-weighted sequence (400–600/11–20) had an 8–10 mm section thickness and a 2 mm gap. The matrix was  $256 \times 128$ –192 with two signals being acquired.

#### **FDG PET/CT**

Twenty-three patients underwent an integrated PET/CT examination. All of the patients fasted for at least six hours before, although oral hydration with glucose-free water was allowed. After ensuring a normal blood glucose level in the peripheral blood, the patients received an intravenous injection of 260–485 MBq of  $^{18}\text{F}$ -FDG and then rested for approximately 45 min before undergoing imaging. Image acquisition was performed using an integrated PET/CT device (Discovery LS; GE Healthcare) consisting of an Advance NXi PET scanner and an 8-slice Light Speed Plus CT scanner. The axes of both systems were mechanically aligned so that shifting the examination table by 68 cm moved the patient from the CT gantry into the PET gantry. The resulting PET and CT images were co-registered on hardware.

The CT was performed from the head to the pelvic floor utilizing a standardized protocol consisting of 140 kV, 80 mA, a tube-rotation time of 0.5 sec/rotation, a pitch of 6 and a section thickness of 5 mm, which matched the PET image section thickness. The patients were in normal shallow respiration during the acquisition of the CT scans and no contrast material was administered. Immediately after the CT, the PET was performed in the identical axial field of view. The acquisition time for PET was 5 minutes per table position. The CT data was resized from a  $512 \times 512$  matrix to a  $128 \times 128$  matrix to match the PET data; thus allowing the images to be fused and CT transmission maps to be generated. The PET image datasets were reconstructed iteratively using the ordered-subsets expectation maximization algorithm. The attenuation correction (2 iterations, 28 subsets) was measured using the CT data. The co-registered images were displayed using the eNTEGRA software (GE Healthcare).

#### **Image Analysis**

The analysis of the MR and integrated PET/CT images was performed retrospectively without any knowledge of the pathological results, serum CA-125 levels, or the results of other imaging examinations. Two genitourinary radiologists (B.K.P. and C.K.K.) assessed the MR images of the abdomen and pelvis in consensus. The PET/CT images were assessed by a nuclear medicine physician (J.Y.C.).

In a patient-based analysis for the presence or absence of peritoneal seeding, the results of the MRI and PET/CT were compared with the histopathological findings following the laparotomies.

For a lesion-based analysis, the peritoneum was divided into six different sites: a) pelvis, b) anterior parietal peritoneum, c) paracolic gutters, d) subphrenic, perihepatic or perisplenic space, e) mesentery and f) omentum.

The diagnostic criteria for peritoneal seeding detected by MRI included: 1) peritoneal implants along the peritoneal cavity, 2) fat or nodular soft-tissue infiltration or bulky pancake-like tumors in the mesentery and greater omentum and 3) irregularly nodular thickening along the mesenteric side of bowel wall (9, 11, 26). Neither ascites alone nor the presence of abdominal or pelvic lymphadenopathy was considered to be peritoneal carcinomatosis.

For the integrated PET/CT, when an abnormal FDG uptake was detected, the precise anatomic location was indicated on the CT scan. As for the integrated PET/CT

images, the entire peritoneum, including the six specific sites, were evaluated for the presence or absence of a tumor. The diagnosis of peritoneal seeding was considered when an abnormal focal uptake observed on the PET images corresponded to an abnormal soft-tissue mass; or an irregularly nodular thickening in the peritoneum of the abdomen and pelvis was detected on CT images (24, 27). Without the findings of abnormal soft-tissue or irregularly nodular thickening in the peritoneum on CT images, peritoneal uptake on the PET images was considered to be negative for peritoneal seeding.

After the MRI and PET/CT findings were independently analyzed, the operative notes and histopathological findings were reviewed, and the presence or absence of peritoneal seedings was recorded in six different sites of the peritoneum, based on the histopathological results. For the lesion-based analysis, the results of the MRI and PET/CT were compared with the histopathological findings.

### Statistical Analysis

The sensitivity, specificity, accuracy, positive predictive value (PPV), and negative predictive value (NPV) for peritoneal carcinomatosis from ovarian cancer were evaluated in 23 patients using MRI and integrated PET/CT. For the patient-based and lesion-based sensitivity and specificity, a comparison between the integrated PET/CT and MRI to diagnose peritoneal carcinomatosis resulting from ovarian cancer was performed using McNemar's test with a Bonferroni correction. A  $p$ -value of less than 0.0083 was considered to indicate a statistically significant difference.

The accuracy values of each reading session for the 138 sites of the 23 patients were analyzed by way of generalized estimation equations to account for clustering effects from multiple measurements in the same patient.  $P$ -values less than 0.05 were considered statistical-

ly significant. Two-tailed tests were used to calculate all  $P$ -values. The statistical analysis was performed using the SAS software (version 8; SAS Institute, Cary, NC U.S.A.).

## Results

The presence of peritoneal carcinomatosis was histopathologically confirmed in 19 (83%) of 23 patients after primary debulking surgery. Eighty-three (60%) of the 138 sites had histopathologically peritoneal seedings [pelvis ( $n = 19$ ), paracolic gutters ( $n = 19$ ), anterior parietal peritoneum ( $n = 5$ ), subphrenic/perihepatic/perisplenic ( $n = 19$ ), mesentery ( $n = 2$ ) and omentum ( $n = 19$ )].

Table 1 shows the patient-based diagnostic accuracy of predicting peritoneal carcinomatosis in 23 patients with ovarian cancer for the integrated PET/CT and contrast-enhanced MRI. The patient-based sensitivity and accuracy for the MRI were 95% and 87% ( $p > 0.05$ ), while the patient-based sensitivity and accuracy for the PET/CT were 84% and 78% ( $p > 0.05$ ), respectively.

Table 2 shows the lesion-based diagnostic results for the detection of peritoneal carcinomatosis in the 138 sites from the 23 patients. The sensitivity of MRI was superior to the sensitivity of integrated PET/CT ( $p = 0.004$ ) (Fig. 1, 2). Overall, the accuracy of MRI was slightly higher than the accuracy of integrated PET/CT, although not statistically significant ( $p > 0.05$ ). The specificity of integrated PET/CT was higher than the specificity of MRI, but again not statistically significant ( $p > 0.05$ ).

Of the false-positive cases for the lesion-based analysis, 9 of them used the integrated PET/CT (Fig. 3). The sites included the anterior parietal peritoneum ( $n = 3$ ), pelvis ( $n = 2$ ), paracolic gutters ( $n = 2$ ) and mesentery ( $n = 2$ ). Similarly, 13 false-positive cases were observed for

Table 1. Patient-Based Diagnostic Performances of the Integrated PET/CT versus MRI for the Preoperative Prediction of Peritoneal Carcinomatosis in 23 Patients

	PET/CT	MRI
Sensitivity (%)	84 (16/19)	95 (18/19)
Specificity (%)	50 (2/4)	50 (2/4)
PPV (%)	87 (16/18)	90 (18/20)
NPV (%)	40 (2/5)	67 (2/3)
Accuracy (%)	78 (18/23)	87 (20/23)

Note.— The numbers in parentheses are the values used to calculate the percentages. PPV = positive predictive value, NPV = negative predictive value

Table 2. Lesion-based Diagnostic Performance of the Integrated PET/CT versus MRI for the Preoperative Prediction of Peritoneal Carcinomatosis in 138 Sites from 23 Patients

	Sensitivity (%)	Specificity (%)	PPV (%)	NPV (%)	Accuracy (%)
PET/CT	75 (62/83)	84 (46/55)	87 (62/71)	67 (46/67)	78 (108/138)
MRI	86 (71/83)	76 (42/55)	85 (71/84)	78 (42/54)	82 (113/138)

Note.— The numbers in parentheses are the values used to calculate the percentages. PPV = positive predictive value, NPV = negative predictive value

the MRI. The sites included the paracolic gutters ( $n = 5$ ), mesentery ( $n = 3$ ), anterior parietal peritoneum ( $n = 3$ ) and pelvis ( $n = 2$ ).

### Discussion

Peritoneal carcinomatosis is the malignant seeding of the peritoneum. It most commonly arises from the ovaries, colon, stomach and pancreas (28, 29). In ovarian cancer, peritoneal seeding is the most common pathway for the spread to other parts of the body. As 90% of ovarian cancers are surface epithelial carcinomas, the tumor cells can slough off the ovary and enter the peri-

toneal circulation to seed multiple sites (30). The intraperitoneal circulation of peritoneal fluid is the main channel directing intraperitoneal seeding. The negative pressure present under the diaphragm along with the increased capillary forces at the dome of the liver quite commonly create metastatic deposits on the liver surface (4). Peritoneal implants are often low in volume and occur in the form of soft tissue masses that appear as solitary or multiple nodules. The nodules can coalesce to form a plaque that coats the viscera. The large omental plaques, referred to as omental cakes (31), appear as areas of irregular soft tissue thickening. Large omental plaques. The common sites of metastases include the

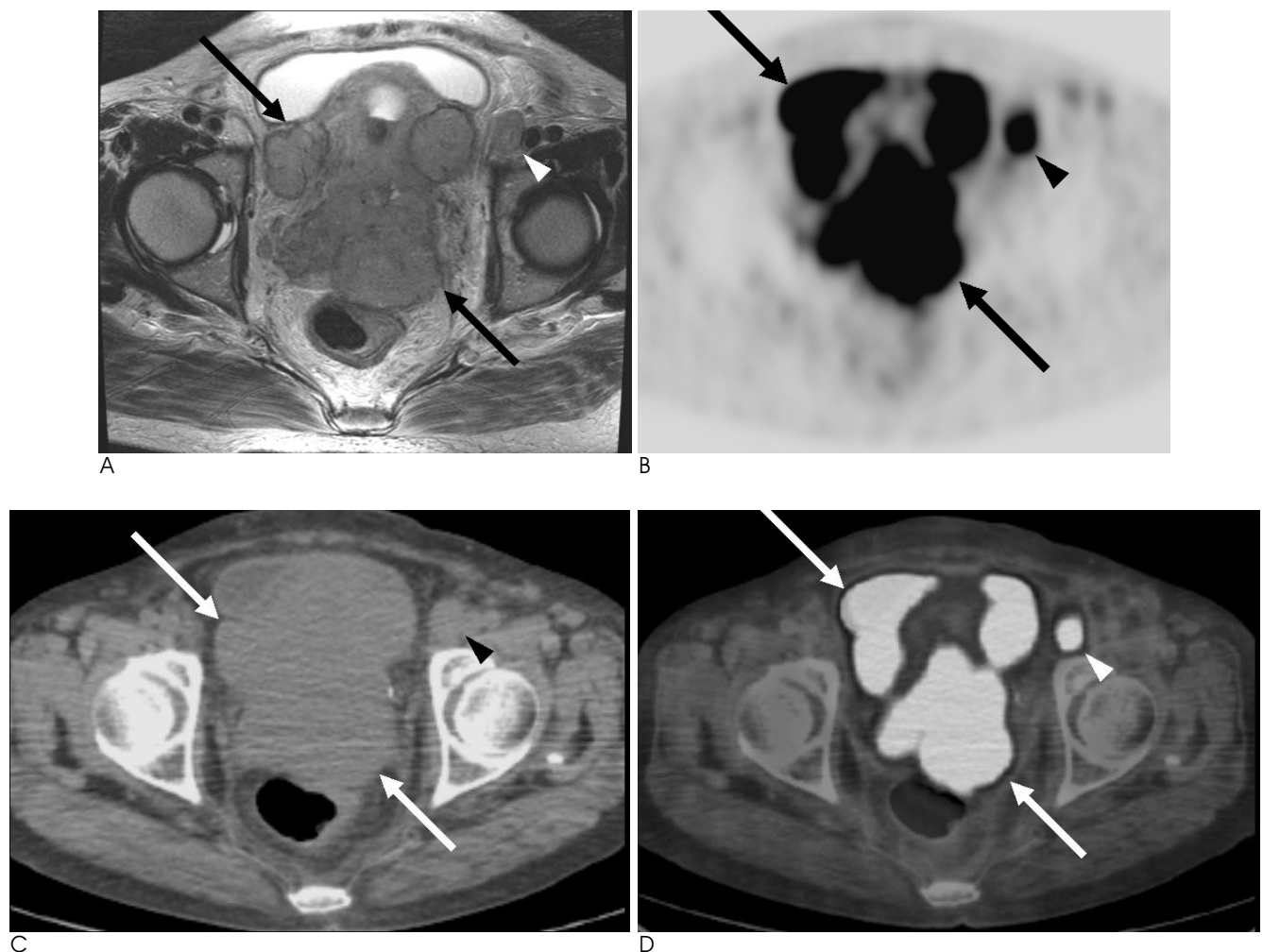


Fig. 1. A 53-year-old woman with stage IIIC ovarian carcinoma and a serum CA-125 level of 563 U/mL.  
A. A transverse T2-weighted image shows large soft-tissue peritoneal implants in the pelvis that are invading the uterus and adnexae (arrows). Note the presence of an enlarged lymph node in the left inguinal region, representing a metastasis (arrowhead).  
B. A FDG PET scan shows metabolically active foci in the pelvis (arrows) and left inguinal area (arrowhead).  
C. A transverse unenhanced CT scan demonstrates the presence of large soft-tissue implants in the pelvis (arrows) and left inguinal region (arrowhead) that correspond to the foci in (B).  
D. A combined PET/CT image shows areas of increased uptake localized to the soft-tissue implants in the pelvis (arrows) and left inguinal region (arrowhead), which confirm the presence of metastatic lesions. The diagnoses of peritoneal carcinomatosis in the pelvis and a metastatic lymph node in left inguinal region were confirmed by the histological findings.

right hemi-diaphragm, liver, right paracolic gutter, bowel, omentum and pelvis (15).

Currently, CT is the primary modality employed for the diagnosis and follow-up of peritoneal carcinomatosis resulting from ovarian cancer. The use of spiral CT has shown a sensitivity of 85–93% and a specificity of 91–96% for the prediction of peritoneal seeding from ovary cancer (12). The advent of the multidetector CT (MDCT) has the potential to improve the CT evaluation of the local extension of the disease. In effect, coronal or sagittal reformatted images facilitate the detection of small lesions, and with fewer artifacts (31). However, until now, there is no published data on the detection of peritoneal

seeding using MDCT.

Although CT is the primary modality used to evaluate an ovarian cancer metastasis, MR imaging has a staging accuracy similar to that of the spiral CT (11). Tempany *et al.* (11) showed that the sensitivity and specificity of a peritoneal metastasis from ovarian cancer performing the contrast-enhanced MRI were 95% and 80%, respectively, compared to the spiral CT which had a sensitivity and specificity of 92% and 82%, respectively. For the advanced stages of ovarian cancer, MRI and spiral CT showed a similar level of accuracy for the determination of the location, distribution and size of the peritoneal seeding. However, in the study, the investigators sug-

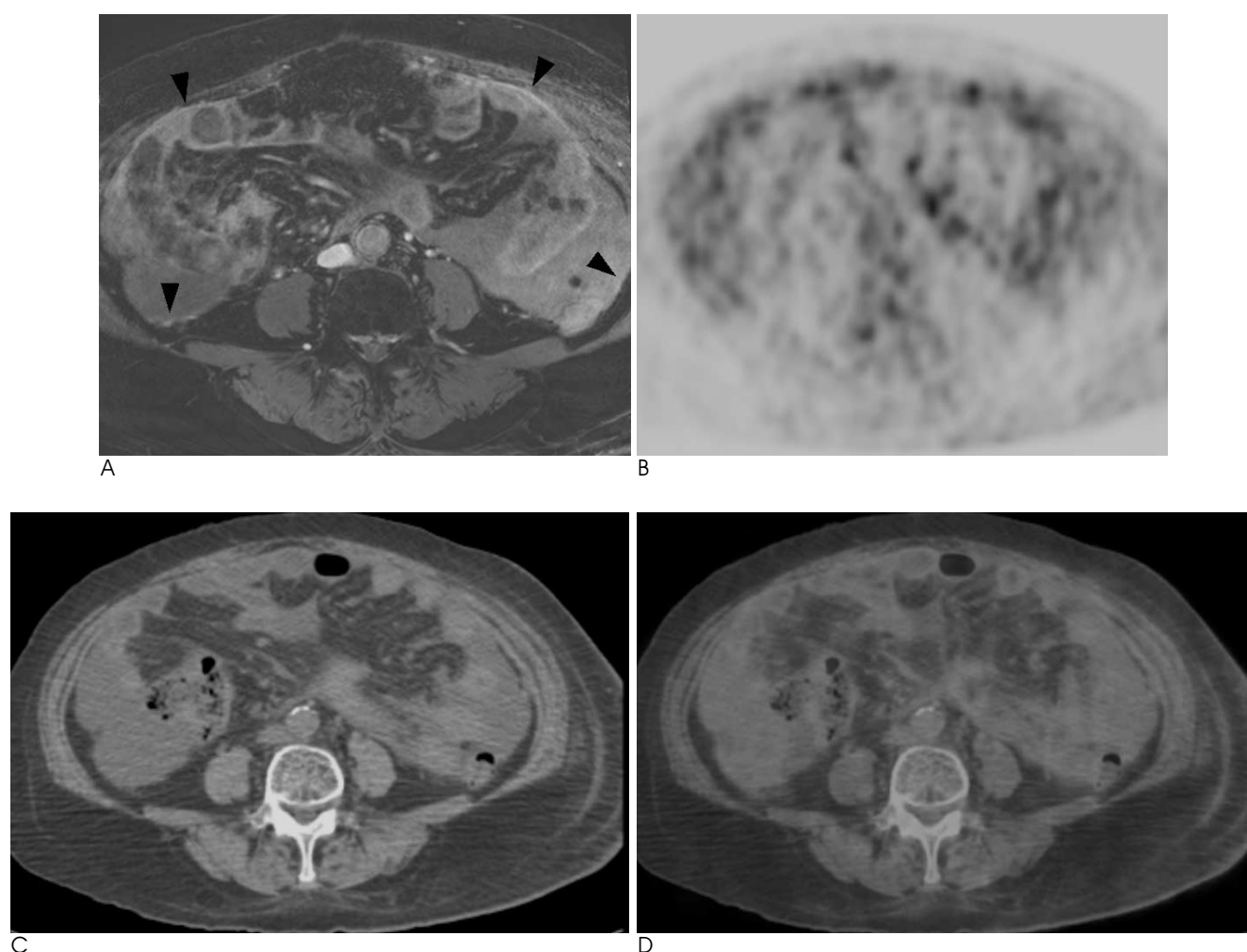


Fig. 2. A 65-year-old woman with stage IIIC ovarian carcinoma and a serum CA-125 level of 368 U/mL.

A. An axial post-contrast fat-saturated T1-weighted image shows diffuse peritoneal thickening and enhancement in the anterior portion of the abdomen and both paracolic gutters (arrowheads). In addition, a small amount of ascites are observed.

B. An axial FDG PET scan shows multiple foci with minimal FDG activity in the anterior portion of the abdomen and both paracolic gutters. The standardized uptake values are 4.4.

C. An axial unenhanced CT scan demonstrates normal-appearing bowel loops with a small amount of ascites. No abnormal soft-tissue implants are seen.

D. An axial integrated PET/CT image shows minimally increased FDG uptake in the anterior portion of the abdomen and both paracolic gutters. These findings are considered as a negative for the diagnosis of peritoneal carcinomatosis.



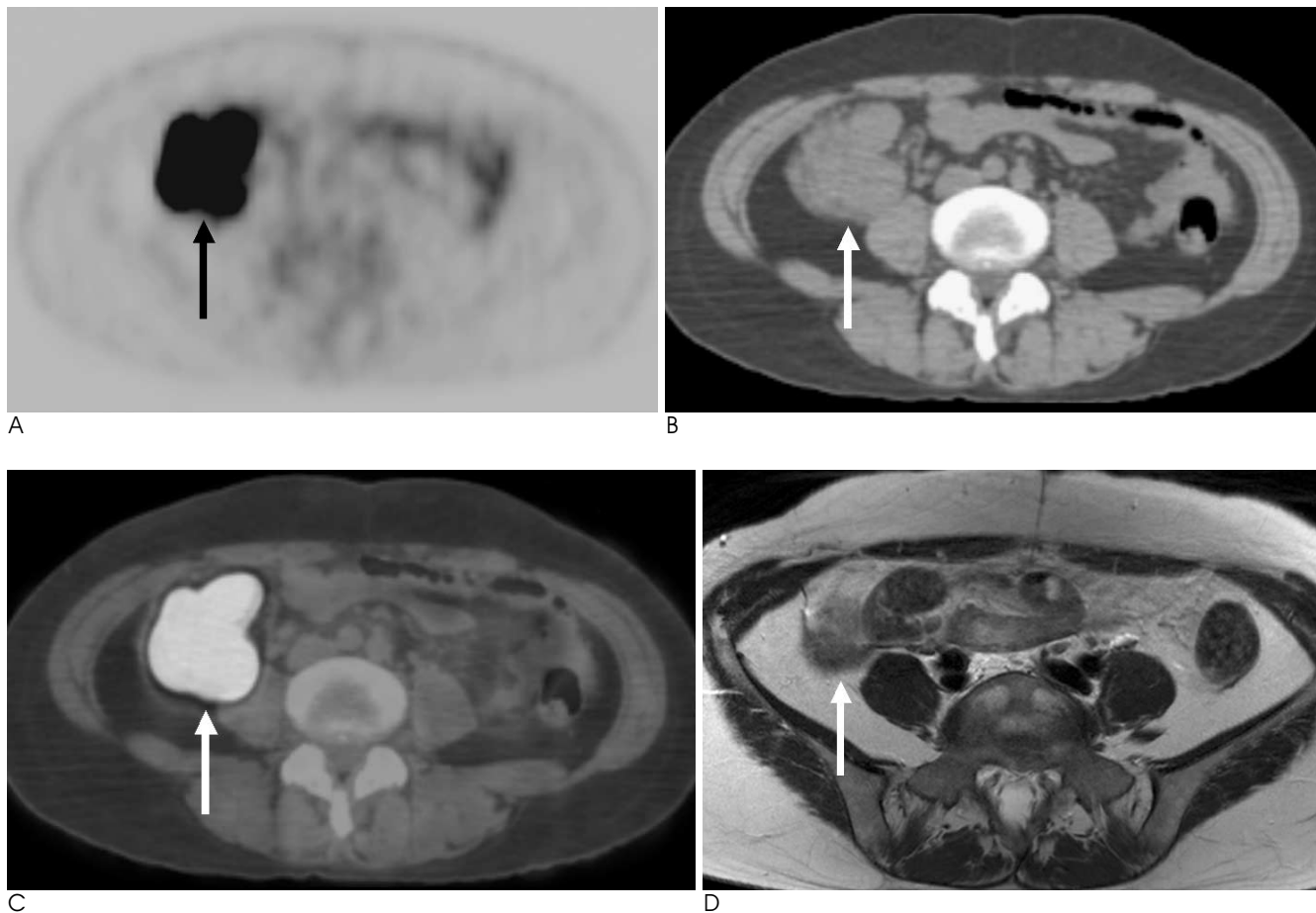


Fig. 3. A 58-year-old woman with stage IIb ovarian carcinoma and a serum CA-125 level of 268 U/mL.  
 A. An axial FDG PET scan shows a focus of metabolically increased activity in the right lower quadrant (arrow). The standardized uptake values are 9.7.  
 B. An axial unenhanced CT scan demonstrates the presence of a soft-tissue lesion (arrow) corresponding to the focus shown in (A).  
 C. An axial integrated PET/CT image shows a focus of increased uptake localized to the soft-tissue lesion in the right lower quadrant (arrow), which represents the presence of a metastatic lesion. However, an axial T2-weighted image (D) shows no abnormal soft-tissue lesion in the right lower quadrant. A normal-appearing cecum (arrow) is seen. During the debulking surgery, no abnormal soft-tissue implant in the right lower quadrant was found. Hence, the focus of increased FDG activity in the right lower quadrant on the integrated PET/CT imaging was normal physiological FDG uptake.

gested that the use of MRI could improve the visualization of small or equivocal peritoneal implants compared to the spiral CT. Low et al (10) reported that the use of double-contrast MRI revealed more peritoneal implants than the spiral CT or unenhanced MRI. In particular, tumors  $\leq 1$  cm in diameter were better detected using the double-contrast MR imaging.

In comparison to CT and MRI, diagnoses with FDG PET are made based on functional rather than morphological criteria. The role of whole body FDG PET in the diagnosis and staging of primary ovarian tumors is still a matter of debate. Early studies have shown sensitivities and specificities of 83-86% and 54-86%, respectively (32, 33). A recent study has demonstrated that the routine use of FDG PET is unsuitable as a diagnostic imaging

procedure for lesion characterization, evaluation of the extent of the disease and the relationship with the adjacent organs (34). More recently, several studies examining the detection of peritoneal carcinomatosis by PET have demonstrated that the use of combined PET and CT showed a sensitivity of 67-78% and a PPV of 92-95% (24, 25).

To the best of our knowledge, no reports have compared the use of integrated PET/CT with MRI for the preoperative depiction of peritoneal carcinomatosis from primary ovarian cancer. In the present study, the lesion-based analysis revealed that the sensitivity of MRI was superior to that of the integrated PET/CT ( $p = 0.004$ ), while the specificity of the integrated PET/CT was superior to that of MRI ( $p > 0.05$ ). The overall accu-

racy of MRI and integrated PET/CT was similar. For the patient-based results of this study, the use of MRI showed a higher sensitivity and accuracy than PET/CT. However, the difference was not statistically significant.

For the present study, the lesion-based analysis of the, the false-positive rate of integrated PET/CT and MRI was 16% and 24%, respectively, whereas for the false-positive findings of the integrated PET/CT, we suggest that low tissue contrast among the internal organs was a cause of the false-positives. In particular, our study indicated that the use of the unenhanced CT may only result in a difficulty to differentiate between physiological uptake of FDG and uptake of FDG by a tumor. For the false-positive cases detected with MRI, 62% (8/13) were located in the paracolic gutters and mesentery, which may be difficult to determine if irregular peritoneal thickening or mesenteric infiltration demonstrates peritoneal seeding or not. In addition, abdominal MR imaging was performed using a breath-hold, however many patients with advanced ovarian cancer might have some difficulty in breath-holding; thus resulting in motion artifacts. Furthermore, many patients with ovarian cancer had massive ascites, which may lead to artifacts. In turn, these artifacts may be a cause of the false-positive findings detected on MRI.

One limitation of this study was that the ability of MRI to detect peritoneal carcinomatosis from primary ovarian cancer in terms of the size of the peritoneal nodule or mass was not compared with that of PET. The size of peritoneal implants is very important for the determination of treatment planning or cytoreduction. Peritoneal implants measuring 2 cm or greater can be debulked with surgery. Attempts to surgically debulk sub-optimal implants (< 2 cm) result in a long-term survival rate below 10% (35, 36). A large prospective study including an analysis of the size of the peritoneal implants will be needed to evaluate accurately peritoneal carcinomatosis from ovarian cancer. Another limitation was that in all patients, an unenhanced CT was used for integrated PET/CT imaging. In a future study, a comparison between the use of integrated PET/CT imaging using contrast-enhanced CT and MRI should be performed for the prediction of peritoneal carcinomatosis. Finally, the number of patients in the study group was very small and the analysis of this study was retrospective.

In conclusion, MRI was more sensitive than integrated PET/CT in the preoperative prediction of the presence of peritoneal carcinomatosis resulting from ovarian cancer. However, the overall accuracy between the two

modalities was not significantly different.

## References

1. National Cancer Information Center. All information about cancer. National Cancer Information Center Web site. Available at: <http://www.cancer.go.kr/cms/statistics/mortality/index.html> Accessed July 2008
2. National Cancer Information Center. All information about cancer. National Cancer Information Center Web site. Available at: <http://www.cancer.go.kr/cms/statistics/incidence/index.html> Accessed July 2008
3. Benedet JL. Progress in gynecologic cancer detection and treatment. *Int J Gynaecol Obstet* 2000;70:135-147
4. Meyers MA. Distribution of intra-abdominal malignant seeding: dependency on dynamics of flow of ascitic fluid. *Am J Roentgenol Radium Ther Nucl Med* 1973;119:198-206
5. Rose PG, Piver MS, Tsukada Y, Lau TS. Metastatic patterns in histologic variants of ovarian cancer. An autopsy study. *Cancer* 1989;64:1508-1513
6. Simojoki M, Santala M, Vuopala S, Kauppila A. The prognostic value of peritoneal cytology in ovarian cancer. *Eur J Gynaecol Oncol* 1999;20:357-360
7. Woodward PJ, Hosseinzadeh K, Saenger JS. From the archives of the AFIP: radiologic staging of ovarian carcinoma with pathologic correlation. *Radiographics* 2004;24:225-246
8. Low RN, Duggan B, Barone RM, Saleh F, Song SY. Treated ovarian cancer: MR imaging, laparotomy reassessment, and serum CA-125 values compared with clinical outcome at 1 year. *Radiology* 2005;235:918-926
9. Low RN, Saleh F, Song SY, Shiftan TA, Barone RM, Lacey CG, et al. Treated ovarian cancer: comparison of MR imaging with serum CA-125 level and physical examination—a longitudinal study. *Radiology* 1999;211:519-528
10. Low RN, Barone RM, Lacey C, Sigeti JS, Alzate GD, Sebrechts CP. Peritoneal tumor: MR imaging with dilute oral barium and intravenous gadolinium-containing contrast agents compared with unenhanced MR imaging and CT. *Radiology* 1997;204:513-520
11. Tempany CM, Zou KH, Silverman SG, Brown DL, Kurtz AB, McNeil BJ. Staging of advanced ovarian cancer: comparison of imaging modalities—report from the Radiological Diagnostic Oncology Group. *Radiology* 2000;215:761-767
12. Coakley FV, Choi PH, Gougoutas CA, Pothuri B, Venkatraman E, Chi D, et al. Peritoneal metastases: detection with spiral CT in patients with ovarian cancer. *Radiology* 2002;223:495-499
13. Ricke J, Sehoul J, Hach C, Hanninen EL, Lichtenegger W, Felix R. Prospective evaluation of contrast-enhanced MRI in the depiction of peritoneal spread in primary or recurrent ovarian cancer. *Eur Radiol* 2003;13:943-949
14. Forstner R, Hricak H, Powell CB, Azizi L, Frankel SB, Stern JL. Ovarian cancer recurrence: value of MR imaging. *Radiology* 1995;196:715-720
15. Forstner R, Hricak H, White S. CT and MRI of ovarian cancer. *Abdom Imaging* 1995;20:2-8
16. Outwater EK, Siegelman ES, Wilson KM, Mitchell DG. Benign and malignant gynecologic disease: clinical importance of fluid and peritoneal enhancement in the pelvis at MR imaging. *Radiology* 1996;200:483-488
17. Low RN, Semelka RC, Worawattanakul S, Alzate GD, Sigeti JS. Extrahepatic abdominal imaging in patients with malignancy: comparison of MR imaging and helical CT, with subsequent surgi-



- cal correlation. *Radiology* 1999;210:625-632
18. Prayer L, Kainz C, Kramer J, Stiglbauer R, Schurawitzki H, Baldt M, et al. CT and MR accuracy in the detection of tumor recurrence in patients treated for ovarian cancer. *J Comput Assist Tomogr* 1993;17:626-632
19. Rose PG, Faulhaber P, Miraldi F, Abdul-Karim FW. Positive emission tomography for evaluating a complete clinical response in patients with ovarian or peritoneal carcinoma: correlation with second-look laparotomy. *Gynecol Oncol* 2001;82:17-21
20. Wang PH, Liu RS, Li YF, Ng HT, Yuan CC. Whole-body PET with (fluorine-18)-2-deoxyglucose for detecting recurrent primary serous peritoneal carcinoma: an initial report. *Gynecol Oncol* 2000;77:44-47
21. Cho SM, Ha HK, Byun JY, Lee JM, Kim CJ, Nam-Koong SE, et al. Usefulness of FDG PET for assessment of early recurrent epithelial ovarian cancer. *AJR Am J Roentgenol* 2002;179:391-395
22. Nakamoto Y, Saga T, Ishimori T, Mamede M, Togashi K, Higuchi T, et al. Clinical value of positron emission tomography with FDG for recurrent ovarian cancer. *AJR Am J Roentgenol* 2001;176:1449-1454
23. Kubik-Huch RA, Dorffler W, von Schulthess GK, Marincek B, Kochli OR, Seifert B, et al. Value of (18F)-FDG positron emission tomography, computed tomography, and magnetic resonance imaging in diagnosing primary and recurrent ovarian carcinoma. *Eur Radiol* 2000;10:761-767
24. Turlakow A, Yeung HW, Salmon AS, Macapinlac HA, Larson SM. Peritoneal carcinomatosis: role of (18F)-FDG PET. *J Nucl Med* 2003;44:1407-1412
25. Suzuki A, Kawano T, Takahashi N, Lee J, Nakagami Y, Miyagi E, et al. Value of 18F-FDG PET in the detection of peritoneal carcinomatosis. *Eur J Nucl Med Mol Imaging* 2004;31:1413-1420
26. Kim CK, Park BK, Choi JY, Kim BG, Han H. Detection of recurrent ovarian cancer at MRI: comparison with integrated PET/CT. *J Comput Assist Tomogr* 2007;31:868-875
27. Pannu HK, Bristow RE, Cohade C, Fishman EK, Wahl RL. PET-CT in recurrent ovarian cancer: initial observations. *Radiographics* 2004;24:209-223
28. Healy JC, Reznick RH. The peritoneum, mesenteries and omenta: normal anatomy and pathological processes. *Eur Radiol* 1998;8:886-900
29. Raptopoulos V, Gourtsoyiannis N. Peritoneal carcinomatosis. *Eur Radiol* 2001;11:2195-2206
30. Ozols RF, Schwartz PE, Eifel PJ. *Ovarian Cancer, fallopian tube carcinoma, and peritoneal carcinoma*. In DeVita VT, Hellman S, Rosenberg SA. *Cancer: principles and practice of oncology*. 6th ed. Philadelphia, Pa: Lippincott Williams & Willins, 2001:1597-1632
31. Pannu HK, Bristow RE, Montz FJ, Fishman EK. Multidetector CT of peritoneal carcinomatosis from ovarian cancer. *Radiographics* 2003;23:687-701
32. Hubner KF, McDonald TW, Niethammer JG, Smith GT, Gould HR, Buonocore E. Assessment of primary and metastatic ovarian cancer by positron emission tomography (PET) using 2-[18F]deoxyglucose [2-[18F]FDG]. *Gynecol Oncol* 1993;51:197-204
33. Romer W, Avril N, Dose J, Ziegler S, Kuhn W, Herz M, et al. [Metabolic characterization of ovarian tumors with positron-emission tomography and F-18 fluorodeoxyglucose]. *Rofo* 1997;166:62-68
34. Rieber A, Nussle K, Stohr I, Grab D, Fenchel S, Kreienberg R, et al. Preoperative diagnosis of ovarian tumors with MR imaging: comparison with transvaginal sonography, positron emission tomography, and histologic findings. *AJR Am J Roentgenol* 2001;177:123-129
35. Cannistra SA. Cancer of the ovary. *N Engl J Med* 1993;329:1550-1559
36. Hoskins WJ. Epithelial ovarian carcinoma: principles of primary surgery. *Gynecol Oncol* 1994;55:S91-96

## 원발성 난소암의 복막 내 암종증의 수술 전 진단에서 MRI와 PET/CT의 비교연구<sup>1</sup>

<sup>1</sup>성균관대학교 의과대학 삼성서울병원 영상의학과

<sup>2</sup>성균관대학교 의과대학 삼성서울병원 핵의학과

김찬교 · 박병관 · 최준영<sup>2</sup> · 김지혜

**목적:** 원발성 난소암으로부터 복막 내 암종증의 수술 전 진단에서 MRI와 PET/CT의 진단적 정확성을 비교하고자 하였다.

**대상과 방법:** 난소암으로 의심되는 23명의 환자에서 수술 전에 조영증강 1.5T MRI와 18F-FDG PET/CT를 시행하였다. 병변 분석을 위해 복강은 6부위로 구분되었다. 영상소견은 병리결과와 비교되었으며, 통계분석은 Bonferroni 교정을 한 McNemar 검사법과 generalized estimation equations법을 사용되었다.

**결과:** 총 23명 환자는 조직병리 결과에서 원발성 악성 상피성 난소암으로 확진 되었다. 23명 중 19명 환자의 총 83 곳에서 복강 내 암종증이 발견되었다. 복강 내 암종증의 발견에 대해서 환자기반 MRI와 PET/CT의 민감도, 특이도 그리고 정확성은 각각 95%와 84% ( $p > 0.05$ ), 50%와 50% ( $p > 0.05$ ) 그리고 87%와 78% ( $p > 0.05$ )였다. 병변기반 MRI와 PET/CT의 민감도, 특이도 그리고 정확성은 각각 86%와 75% ( $p = 0.004$ ), 76%와 84% ( $p > 0.05$ ) 그리고 82%와 78% ( $p > 0.05$ )였다.

**결론:** 원발성 난소암으로부터 복강 내 암종증을 수술 전에 진단하는데 있어 MRI는 PET/CT보다 민감하였다.